A Novel Potassium Channel Blocking Toxin from the Scorpion *Pandinus imperator*: A ^{1}H NMR Analysis Using a Nano-NMR Probe†

M. Delepierre,*,‡ A. Prochnicka-Chalufour,‡ and L. D. Possani§

Laboratoire de Résonance Magnétique Nucléaire, Institut Pasteur, CNRS URA 1129, 28 rue du Dr. Roux, 75724 Paris Cedex 15, France, and Department of Molecular Recognition and Structural Biology, Institute of Biotechnology, National Autononous University of Mexico, Avenue Universidad, 2001 Cuernavaca, Mexico 62271

Received July 12, 1996; Revised Manuscript Received December 17, 1996⊗

ABSTRACT: The three-dimensional solution structure of a novel peptide, Pi1, purified from the venom of the scorpion *Pandinus imperator* and specific for potassium channels was determined by homonuclear proton NMR methods at 500 MHz from nanomole amounts of compound. *P. imperator* toxin is a voltage-dependent potassium channel specific peptide capable of blocking the shaker B K^+ channels expressed in Sf9 cells in culture (*Spodoptera frugiperda* cell line no. 9) and displacing labeled noxiustoxin from rat brain synaptosomal membranes. The toxin has only 35 amino acid residues but is stabilized by four disulfide bridges (Cys4−Cys25, Cys10−Cys30, Cys14−Cys32, and Cys20−Cys35) instead of three commonly found in small potassium channel toxins. A detailed nuclear magnetic resonance structure of this protein was obtained using a nano-NMR probe and a combination of two-dimensional proton NMR experiments. The dihedral angles and distance restraints obtained from measured NMR parameters were used in structural calculations in order to determine the solution conformation of the toxin. The structure is organized around a short α-helix spanning residues Ser8−Thr18 and a β-sheet. These two elements of secondary structure are stabilized by two disulfide bridges, Cys10−Cys30 and Cys14−Cys32. The antiparallel β-sheet is composed of two strands extending from Asn22 to Cys32 with a tight turn at Arg28−Met29 in contact with the N-terminal fragment Leu1−Cys4. Comparison between the 3D structure of Pi1 and those of other structurally and functionally related scorpion toxins is presented.

Scorpion venoms are rich sources of different classes of peptides that affect the function of ion channels (Catterall, 1980). These peptides disrupt the normal function of excitable tissues found in muscles and nerves of many animals, including man, by causing respiratory and circulatory damages that can eventually lead to death. Apart from the important public health problem caused by scorpion stings in certain areas of the world, these peptides represent useful tools for biological research, mainly that concerning cellular excitability and ion channels.

Several toxins have been extensively studied with respect to their structure, mode of action, and localization of the functional site. The most widely known are those specific for sodium and potassium channels (Zlotkin et al., 1978; Rochat et al., 1979; Carbone et al., 1982; Possani et al., 1982; Possani, 1984; Miller et al., 1985; Lazdunski et al., 1986; Meves et al., 1986; Moczydlowski et al., 1988; Blaustein et al., 1991). However, peptides that recognize calcium (Valdivia et al., 1992) and chloride channels (Debin et al., 1993; Lippens et al., 1995) have also been reported. The toxins affecting the sodium channel are, by far, the more important ones in scorpionism whereas toxins affecting the potassium, calcium, and chloride have only a minor contribution to human intoxication (Valdivia et al., 1992; Calderon-Aranda et al., 1995). This is partly due to the fact that the latter are the less abundant components of the venom but also because they are present in scorpion species not dangerous to humans.

Although toxins against sodium and potassium channels differ greatly in their number of amino acids, their three-dimensional structure presents a common motif: a short segment of α-helix and two or three strands of β-sheet, stabilized by two disulfide bridges (Kopeyan et al., 1974; Sugg et al., 1990; Kobayashi et al., 1991; Menez et al., 1992). These segments of the primary structure seem to be responsible for the formation of the motif underlying the main structural core of the scorpion toxins. On the basis of these structural features, two distinct families of peptides were described: the first one with four disulfide bridges contains 61−70 amino acids residues and is active against sodium channels (Zlotkin et al., 1978; Rochat et al., 1979; Possani 1984; Valdivia et al., 1991); the second is represented by short peptides of about 29−39 amino acids, containing three disulfide bridges in the case of toxins specific to mammalian potassium channels (Kopeyan et al., 1974; Carbone et al., 1982; Possani et al., 1982; Miller et al., 1985; Menez et al., 1992) and four disulfide bridges in the case of insectotoxins of which the specificity is not well characterized but presumably linked to the glutamate receptor of the postsynaptic membrane (Grishin et al., 1978; Zlotkin et al., 1978; Rochat et al., 1979; Fazal et al., 1989).

The potassium channel specific toxins can act on (i) the voltage-dependent potassium channels (Kv types, Shaker), (ii) the large conductance, calcium-activated potassium channels (maxi-K or BK-type), and (iii) the small conduc-

† The work in Mexico was supported in part by grants from the Howard Hughes Medical Institute (75191-527104), the European Commission (CI1-CT 94-0045), and the National University of Mexico (DGAPA-IN206994) to L.D.P. The work in Paris was supported by funds from the Pasteur Institute and the Centre National de la Recherche Scientifique.

* Correspondence to this author: email, murield@pasteur.fr.
‡ Institut Pasteur.
§ National Autononous University of Mexico.

⊗ Abstract published in *Advance ACS Abstracts,* February 1, 1997.

S0006-2960(96)01711-4 CCC: $14.00

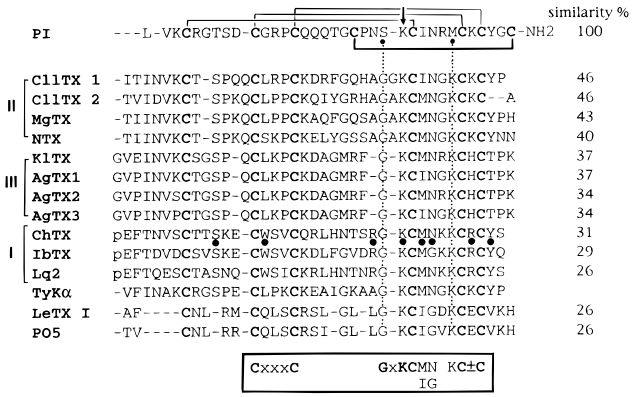

FIGURE 1: Comparison of amino acid sequences and disulfide pairing of Pi1 (PI) with other related potassium channel toxins: ClITX1, ClTX2 (Martin et al., 1994), MgTX (Garcia-Calvo et al., 1993), NTX (Possani et al., 1982), KlTX (Crest et al., 1992), AgTX1,2,3 (Garcia et al., 1994), ChTX (Gimenez-Gallego et al., 1988), IbTX (Galvez et al., 1990), Lq2 (Luchesi et al., 1989), TyKα (Rogowski et al., 1994), LeTx1 (Chicchi et al., 1988; Auguste et al., 1990), and PO5 (Meunier et al., 1993). The eight most important residues involved in the interaction with the channel in the charybdotoxin-like toxins are indicated with black dots. The consensus sequence is boxed whereas the essential lysine for tight binding to the receptor is shown with an arrow. Gaps were introduced to enhance identity.

tance, calcium-dependent potassium channels or apamin sensitive (insectotoxins). The α/β fold adopted by scorpion toxins is capable of exerting a wide functional variability. However, the detailed structural basis for this variability is still poorly understood. This is mainly due to the fact that the potassium channel toxins are always found as minor components of the venoms, often less than 0.5% (Possani et al., 1982; Calderon-Aranda et al., 1995). This has considerably slowed down pharmacological studies of the potassium channels.

Noxiustoxin, a toxin specific for K channels, was first isolated 16 years ago (Possani et al., 1982), but its solution structure was solved only last year (Dauplais et al., 1995). Since the middle of the 1980's, a large number of homologous peptides from scorpions, able to block potassium channels, were identified (Figure 1). All the toxins characterized so far and specific for mammalian potassium channels share obvious sequence similarities and fall into four groups (Miller, 1995). The charybdotoxin-like (ChTX)[1] group, which includes also the iberiotoxin (IbTX) and the leiurus toxin (lq2), potently blocks high-conductance calcium-activated potassium channels (BK channels). The noxiustoxin-like (NTX) group, including the margatoxin MgTX, has a small residue insertion between glycine 26 and lysine 27. The kaliotoxin-like (KTX) group, which includes the agitoxins AgTx1,2,3, has a point deletion between the third and fourth cysteines. The latter and the noxiustoxin-like toxins block the voltage-dependent channels (Kv channels, shaker, and Kv1.3). Finally, the last group, tytiustoxin-type, is represented by only one peptide, thus far (Rogowski et al., 1994).

Here we describe the solution structure of a new class of toxin that blocks potassium channels. This peptide was isolated from the venom of the scorpion *Pandinus imperator*, a Scorpionidae from the Chactoidae subgroup, not dangerous to humans (Sissom, 1990). This scorpion, living in equatorial Africa, is the biggest one to exist and can measure up to 20 cm. The peptide has only 35 amino acid residues but is cross-linked by four disulfide bridges instead of the three commonly found. The pairing of the four disulfide bridges was identified from enzymatic cleavage followed by amino acid and peptide sequence analysis (Olamendi-Portugal et al.,1996). Pairings 4−25, 10−30, and 14−32 correspond to the usual pattern found in short-chain scorpion toxins. The disulfide bridge at position Cys20−Cys35 is the novel structural characteristic of this toxin. This position differs from that occupied by the fourth disulfide bridge of insectotoxins which is located in the N-terminal part of the molecule (Grishin et al., 1978; Debin et al., 1993). The Pi1 toxin reversibly blocks the shaker B potassium channel, which is a voltage-dependent channel, and displaces the binding of [^{125}I]noxiustoxin, a potassium channel blocker from the rat brain synaptosomal membrane with an IC_{50} of about 10 nM (Olamendi-Portugal et al., 1996).

P. imperator toxin 1 is the first potassium channel blocking peptide isolated from scorpion venom that contains four disulfide bridges. For all the reasons mentioned before, and because these toxins represent valuable tools for probing the structure of potassium channels, we found it important to investigate the three-dimensional structure not only to understand its mode of action but also to clarify its functional differences with respect to other potassium channel toxins. The very limited sample quantity, about 50 nmol (approximatively 150 μg), made it impossible to perform the structural analysis using standard NMR technology. We have turned instead to the new experimental possibilities offered by the nano-NMR probe.

This paper deals with the Pi1 ^{1}H NMR assignments, the secondary structure determination, and the calculation of the global 3D structure. The structure obtained is subsequently compared with the structure of other functionally related toxins affecting the potassium channels.

MATERIALS AND METHODS

Sample Preparation. The venom was collected and prepared in the laboratory by electrical stimulation of anesthesized animals (Dent et al., 1980). The *P. imperator* toxin 1 was purified according to the method already described and using analytical grade chemicals only (Olamendi-Portugal et al., 1996). The lyophilized powder, 150 μg, was dissolved in 40 μL of H_2O/D_2O, 9:1 (v/v) (Eurisotop). Taking into account the presence of salt, the toxin concentration was between 0.8 and 1 mM in H_2O, and the solution pH was estimated to be 3−3.5. The pH could not be measured because of the very limited sample size. A unique sample of Pi1 extracted from the venom of about 100 scorpions was used for all NMR measurements.

NMR Spectroscopy. ^{1}H NMR experiments, using a nano-NMR probe (Varian), were run at 500 MHz on a Varian Unity spectrometer with an on-line Sun Sparc 2 workstation. The nano-NMR probe produces high-resolution spectra from liquid samples of 40 μL (Manzi et al., 1995). The coil is placed very close to the sample inside the dewar. This allows one to obtain a better filling factor and subsequently better signal to noise ratio and shorter pulses. The 90° pulse varied between 3.5 and 5 μs for the experiments reported here. The

[1] Abbreviations: NMR, nuclear magnetic resonance; 2D, two dimensional; NOE, nuclear Overhauser effects; NOESY, NOE spectroscopy; COSY, correlated spectroscopy; TOCSY, total correlated spectroscopy; DQ-COSY, double-quantum spectroscopy; rmsd, root-mean-square deviation; ChTX, charybdotoxin, IbTX, iberiotoxin, KTX, kaliotoxin, MgTX, margatoxin, NTX, noxiustoxin, ClTX, chlorotoxin, Pi1, *Pandinus imperator* toxin 1.

Table 1: ^{1}H Chemical Shifts for the *P. imperator* Toxin 1 at 35 °C

	NH	Hα	Hβ Hβ	Hγ	Hδ	Hε	others	J_{NH-Ha}	ppb/°C
1L	(9.60)	4.12	1.79	1.70	0.99			9	
2V	8.97	4.19	1.83	0.99−0.94				9.5	7.7
3K	8.34	4.89	1.75−1.87	1.50	1.72	3.01	7.55	7.6	5.3
4C	8.01	4.83	3.32−3.10					8.5	2
5R	9.17	4.43	1.84−1.92	1.68	3.24		7.37	9.9	1
6G	7.89	4.42−4.03							2.7
7T	9.02	3.66	4.22	1.30				<3	7.3
8S	8.95	4.26	4.02−3.94					<3	8.7
9D	7.67	4.56	2.94−2.88					5.25	2
10C	7.90	4.71	3.12−3.08					weak	2.7
11G	7.45	4.08−3.98							0
12R	8.66	4.37	1.92−1.73	1.61	3.25		7.20	<3	4
13P		4.45	1.82−2.37	2.18−2.06	3.80−3.60				
14C	8.17	4.73	3.46−3.01					5	2.7
15Q	9.01	3.64	2.30−2.18	1.99−1.73				<3	2
16Q	8.30	3.99	2.25−2.19	2.53−2.41				4	1.3
17Q	7.83	4.24	2.23−2.23	2.60−2.37				4.8	2.7
18T	8.37	4.82	4.49	1.27				large	2.7
19G	8.24	4.78−3.80						large	2
20C	8.24	5.18	3.75−2.20					medium	2
21P		4.63	2.08	1.93	3.80−3.56				
22N	(9.60)	4.49	2.90						
23S	8.55	5.25	4.31−3.35					7.4	4.7
24K	8.30	4.61	1.75−1.56	1.40	1.93	3.03	7.55	7.8	1.4
25C	8.38	4.93	2.54−2.89					medium	4
26I	8.92	4.30	1.74	1.41	0.88−0.93			9	1
27N	9.35	4.33	3.06−2.75					6.1	7.3
28R	8.37	3.86	2.18−1.61	2.30	3.23−3.27		7.15	medium	5.4
29M	7.75	5.22	1.90−2.03	2.60−2.49		2.08		9	1
30C	8.86	4.76	2.88−2.56					5	6.7
31K	9.09	4.49	1.80−1.61	0.89−1.08	1.55	2.92−2.75	7.53	10.5	2.7
32C	8.69	4.81	3.62−2.60					8.1	6.7
33Y	8.08	4.51	2.43−3.27		6.95	6.65		7	2.7
34G	9.45	4.32−3.86						5.1	5.6
35C	8.75	4.55	2.88−3.25				7.70−6.98	6.6	6.7

probe uses a solenoidal coil to maximize the available sensitivity and spins samples rapidly (1−3 kHz) at the magic angle to remove the magnetic susceptibility contributions to the ^{1}H NMR line widths (Mozurkevitch et al., 1979; Barbara, 1994). The experimental data were processed using VNMR 5.1 program. The spectral width varied from 5999.7 to 8000 Hz depending on the spinning rate used. Spectra were referenced to the water signal at 4.79 ppm at 25 °C and at 4.63 ppm at 40 °C [relative to 3-(trimethylsilyl)-[2,2,3,3-$^2H_4$]propionate (TMSP), the external reference]. Quadrature detection was employed in all experiments with the carrier frequency always maintained at the solvent resonance. The 2D ^{1}H NMR spectra were recorded in the phase-sensitive mode (States et al., 1982) with 2K or 4K data points, depending on the spectral width, in the t_2 dimension and 512 t_1 increments. A total of 32 or 48 scans were acquired for the COSY, TOCSY, and double-quantum experiments and 64 or 128 scans for the NOESY experiments. Zero-filling was applied prior to Fourier transformation, and data were processed with shifted sine bell window functions in both dimensions, except for the COSY spectra which were apodized with sine bell functions. The strong signal from the solvent (HDO and H_2O) was suppressed by low-power selective irradiation during the recycling delay and, for NOESY spectra, during the mixing period.

Identification of spin systems was obtained through analysis and comparison of two-dimensional P.COSY (Marion & Bax, 1988), Clean TOCSY (Braunschweiler & Ernst, 1983; Bax & Davies 1985; Griesinger et al., 1988), DQ COSY (two-dimensional double-quantum spectroscopy; Boyd et al., 1983), and NOESY (Kumar et al., 1980) spectra recorded at 25, 30, 35, and 40 °C. TOCSY spectra were recorded using the MLEV-17 pulse scheme for the spin lock preceded by a 2 ms trim pulse and with 30, 40, 60, and 80 ms isotropic mixing periods. The double-quantum experiment was optimized for a 15 Hz coupling constant. NOESY spectra were acquired with mixing times of 80, 100, 150, 200, and 250 ms. Peak volumes were evaluated on NOESY spectra acquired with a mixing time of 200 ms. To suppress the residual water signal in NOESY spectra, a post-acquisition treatment, that is time−domain data convolution, has been applied (Sodano et al., 1993).

NH−CαH coupling constants were measured directly from the one-dimensional spectrum obtained with a digital resolution of 0.18 Hz per data point after one zero-filling.

Structure Calculations. Analysis of the obtained NOESY spectra yielded a set of 177 restraints which were classified into three groups defined by the lower limit of 0.18 nm and the upper limits of 0.25, 0.35, and 0.5 nm for the weak, medium, and strong groups, respectively. Among the 91 interresidue restraints 53 were sequential, 6 were between the *i*, *i*+2 pairs of residues, 8 were between the *i*, *i*+3 and *i*, *i*+4 pairs, and 24 corresponded to interactions between pairs further than 4 residues apart. Additional distance constraints have been introduced corresponding to the four disulfide bridges found in the Pi1 toxin.

Twenty-eight Φ dihedral angle restraints were obtained from direct measurements of the $^3J_{NH-H\alpha}$ coupling constants (Pardi et al., 1984). The Φ angles corresponding to $^3J_{NH-H\alpha}$ values ranging from 7 to 9.5 Hz were restrained to the intervals centered around −120° and those with ^3J below 7 Hz to the intervals centered around −70°.

The distance constraints, together with the set of 28 Φ dihedral angle restraints, were taken into account for the

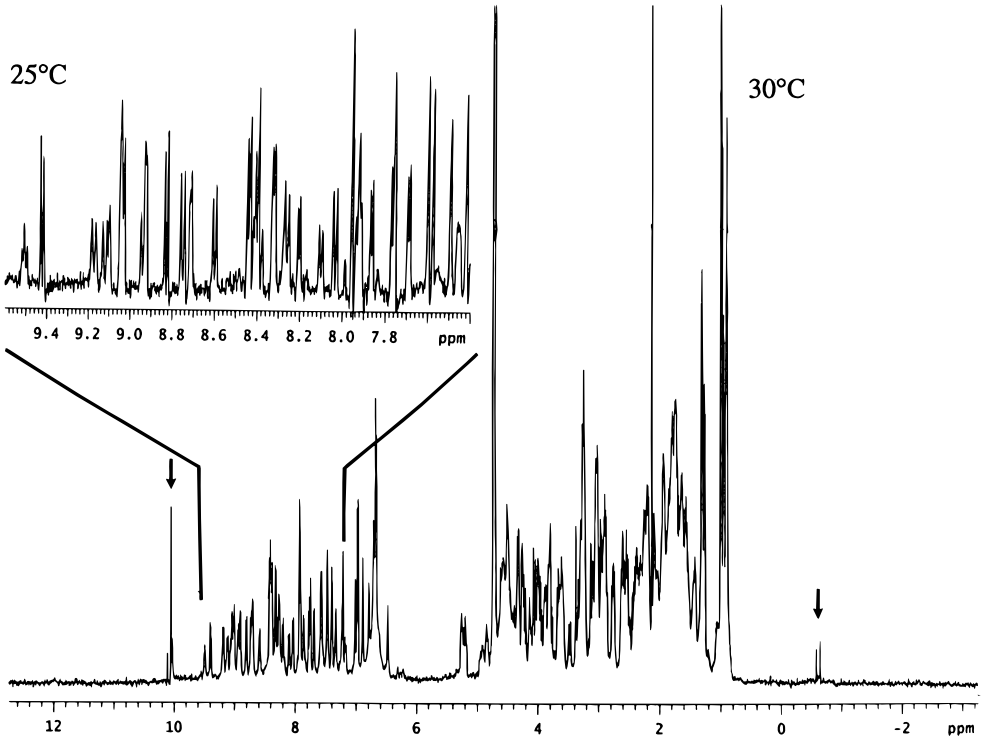

FIGURE 2: One-dimensional proton spectrum of the Pi1 toxin obtained with the nano-NMR probe. The spinning rate is 2650 Hz, and the spinning side bands are indicated with an arrow. The left inset displays the amide proton region.

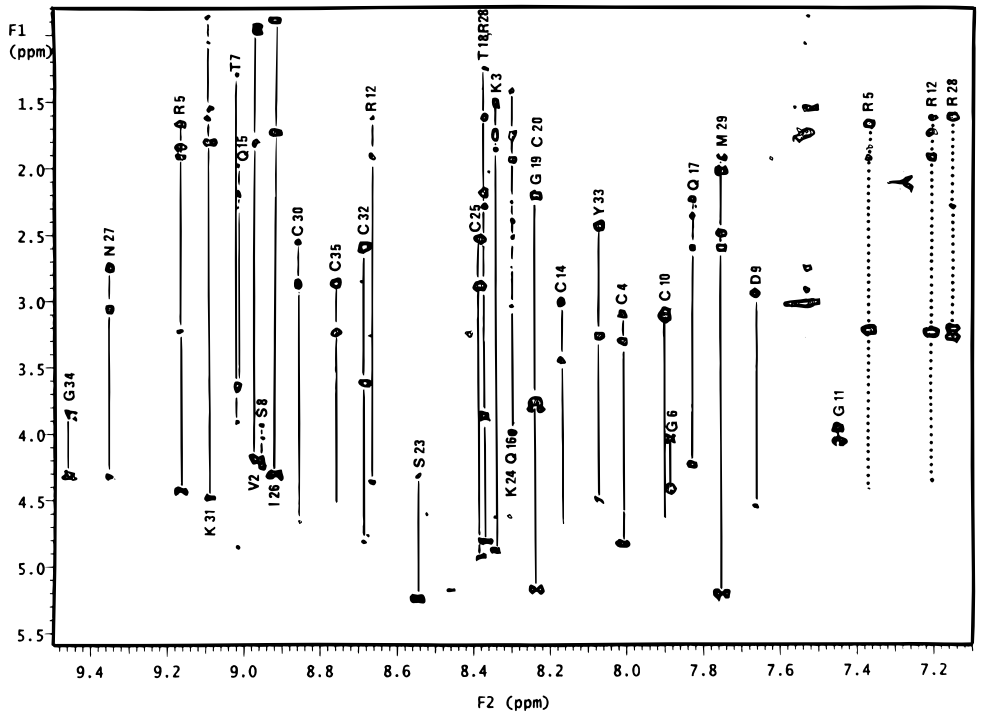

FIGURE 3: Contour plot of a TOCSY spectrum of Pi1 obtained at 35 °C. Spin systems are labeled with the sequential residue position, and a line connects the full spin system.

calculation of initial structures carried out with DIANA software (Güntert et al., 1991), which were used for solving ambiguities or correcting assignments.

Following these preliminary calculations, a hydrogen bond 24:NH-31:O was found in 90% of the 40 structures with the lower target function values. This hydrogen bond, located in a part of the toxin identified as a β-sheet, was compatible with a low value of the corresponding temperature coefficient measured for the amide proton (Table 1). It was therefore included into the set of constraints applied subsequently in structure calculations performed with DIANA using the redundant dihedral angle constraints strategy, REDAC (Güntert & Wüthrich, 1991). Four cycles of REDAC were carried out with the maximal target function value per residue for locally acceptable segments set at 0.4 Å. Of the last 70 structures generated by DIANA, 43 structures had a target function value lower than 1.0 with a total of 13 distance violations greater than 0.3 Å.

Since the total number of available constraints was relatively small, we limited our interest to obtaining overall information about the structure of Pi1. The 20 structures with the lowest value of the target function taken from the

final structures calculated by DIANA were subsequently subjected to constrained energy minimization carried out with the cvff force field in the DISCOVER 95.0 program (Biosym/MSI, San Diego, 1995). The minimization started by 100 steps of steepest descent algorithm followed by two stages of 500 steps of conjugate gradient. A Lenard−Johnson function and a cutoff of 14 Å were used for the van der Waals energy term, and a Morse function for the bond term was used. The set of constraints from the last DIANA calculations was used during the first 500 steps of the minimization, whereas the last 500 steps were carried out with an ensemble of constraints enlarged by four additional hydrogen bonds, persistently appearing in final DIANA structures and consistent with the ensemble of the data. Those were the hydrogen bonds between the HN and O pairs of atoms of residues 11 and 9, 18 and 14, and 31 and 24.

RESULTS

The sequence-specific assignments of Pi1 were achieved according to the two-step standard procedure (Wüthrich, 1986). Spectra were recorded at four different temperatures, namely, 25, 30, 35, and 40 °C, to solve ambiguities due to overlapping signals. The one-dimensional spectrum obtained with presaturation of the water signal shows that good line shape, sensitivity, and resolution can be achieved (Figure 2). In addition, as shown in the left inset, an excellent dispersion of signals is observed in the amide proton region, rendering spin system identification much easier. Finally, some minor peaks are observed which have not been identified so far.

Spin-System Identification. First, the spin systems of all amino acid residues were identified via their through-bond connectivities observed in COSY, TOCSY, and double-quantum experiments. The double-quantum experiment was particularly useful for identification of the NH−Hα connectivities hidden by the strong water signal. It was easy to identify and directly assign the unique spin systems of leucine, valine, isoleucine, and methionine from the TOCSY experiment. Similarly, the six long basic side chains, three arginines and three lysines, were readily assigned due to their characteristic TOCSY lines (Figure 3). By combining the through-bond information acquired at several temperatures, all spin systems, with the exception of one amide proton, Asn22, could be identified.

The protein contains three glutamines and two asparagines. The TOCSY spectrum indicates the existence of two extra cross peaks in the amide region, suggesting an amidation of the C-terminal residue. This is further confirmed in the NOESY spectra in which only the amide proton pair resonating at 7.90 and 6.98 ppm gives an NOE interaction with the Hβ proton of cysteine 35 (data not shown). In the original sequence data published by Olamendi-Portugal et al. (1996) this amidated cysteine at the C-terminus was not detected.

Sequential Assignments. The sequential assignment was obtained using the through-space connectivities NHi−NHi+1, Hαi−NHi+1, and Hβi−NHi+1 observed between neighboring residues in the NOESY spectra. The NOESY spectrum contains some artifacts appearing as spurious cross peaks aligned parallel to the diagonal and due to spinning side bands (not shown). This inconvenience can be easily overcome by changing the spinning rate or the temperature.

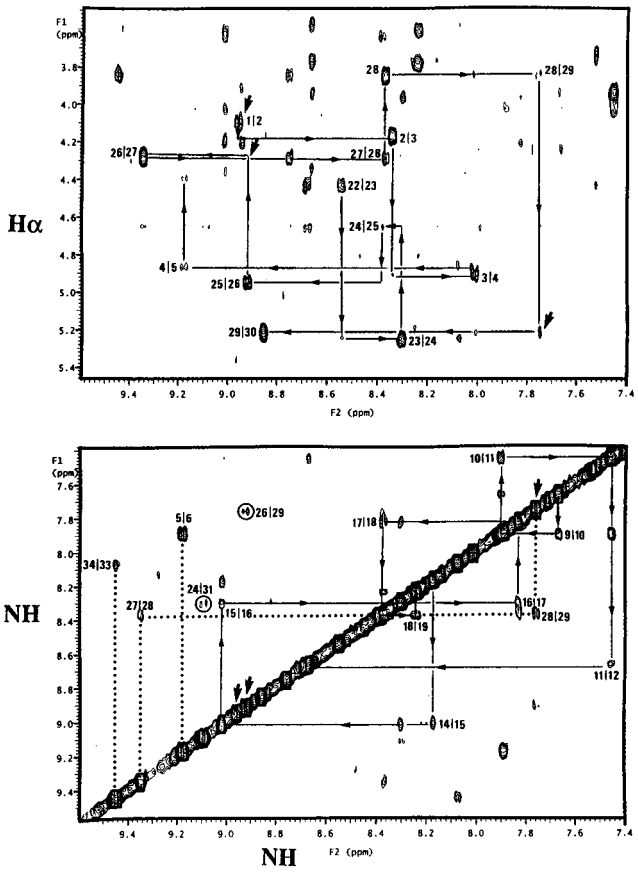

FIGURE 4: NOESY spectrum recorded with 250 ms mixing time at 35 °C. (Top) Contour plot of the fingerprint region. The $d_{\alpha N}$ connectivities are illustrated by lines. (Bottom) Contour plot of the amide region. The sequential d_{NN} connectivities for residues 9−18 are illustrated by a continuous line while dotted lines indicate d_{NN} connectivities involved in turns. The two interstrand d_{NN} interactions are boxed.

The four unique spin systems Leu1, Val2, Ile26, and Met29 were used as starting points for the sequential assignment. In most cases, when the train of sequential Hαi−NHi+1 NOE connectivities is interrupted, the connection is formed by a sequential NHi−NHi+1 NOE, indicating a change in the local secondary structure (Figure 4). The sequential amide or Hα proton NOE connectivities of Arg12 and Cys20 with the Hδ protons of Pro13 and Pro21, respectively, indicate that both Xaa−Pro amide bonds are in the *trans* conformation in the major isomer. The chemical shifts of all protons of Pi1 are listed in Table 1. It is interesting to note that the Asn22 amide proton has not been found. Assuming that this proton might exchange more rapidly with water and was not seen due to the presaturation of the water peak, a one-dimensional spectrum using a soft pulse to suppress the water peak was acquired. Only one extra peak resonating at 9.60 ppm was observed in the spectrum (data not shown). Taking into account the low-field position of this new amide proton resonance, it can be assigned to either the N-terminal residue Leu1 or to Asn22. In Table 1 it is also interesting to note that some of the Lys31 side chain protons are upfield shifted compared to their positions in random coil structures. This suggests that these protons are in close proximity to an aromatic ring. Furthermore, the two Hγ and the two Hϵ protons of the Lys31 side chain each give two distinct resonances, implying that this side chain occupies a well-defined position in the structure as confirmed from the long-range interactions observed between the NH_3 side chain protons with one of the Cys20 Hβ protons.

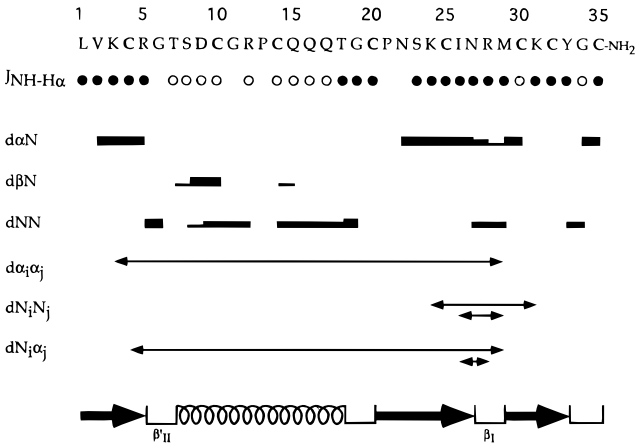

FIGURE 5: Amino acid sequence of Pi1 with a summary of the NOE connectivities used in the sequential assignment procedure and secondary structure determination. Data are summed up from NOESY spectra obtained at 35 °C, pH 3.5, using a mixing time of 200 ms. For proline, sequential NOEs involving CδH instead of NH are indicated. $^3J_{HN\alpha}$ coupling constants greater than 5.5 Hz are represented by filled circles, while open circles correspond to coupling constants lower than 5.5 Hz.

Secondary Structure. The regular secondary structure elements identified on the basis of characteristic sets of specific and short interproton distances and coupling constant analysis are presented in Figure 5. First, the pattern of short-range NH*i*−NH*i*+1 NOEs associated to weak Hαi−NH*i*+1 connectivities together with the $^3J_{HN-H\alpha}$ coupling constants smaller than 5.5 Hz indicated the presence of an α-helix extending from residue 8 to residue 17/18. In addition, weak, typical medium-range cross peaks Hαi−NH*i*+3 (7−10, 8−11, and 13−16) Hαi−Hβi+3 (12−15) could be also observed. A proline insertion in the middle of the helix causes some distortion in the regular pattern as shown in the slightly higher *J* values measured for some of the residues, namely, Asp9 and Cys14.

A three-stranded antiparallel β-sheet can be identified in the Leu1−Cys4, Asn22−Asn27, and Met29−Cys32 segments which exhibit strong sequential α H*i*−NH*i*+1 NOEs indicative of extended conformation. The last two stretches are connected by the Asn27−Met29 fragment which displays several NH*i*−NH*i*+1 connectivities characteristic of a tight turn. The two sequential NH*i*−NH*i*+1 cross peaks detected between residues Asn27 and Arg28 and between Arg28 and Met29 together with the weak sequential Hαi−NH*i*+1 interactions observed between residues Asn27 and Arg28 and between Arg28 and Met29 are an indication of a type I β-turn. This conclusion is reinforced by the information obtained from the $^3J_{HN-H\alpha}$ coupling constant values. A number of long-range NH*i*−NH*j* [24:31; 26:29], α H*i*−NH*j* [23:33], NH*i*−α H*j* [4:29], and α H*i*−α H*j* [3:29] connectivities suggest that the structure is a triple-stranded antiparallel β-sheet. However, the lack of other expected long-range interactions is inconsistent with the formation of a canonical β-strand structure; therefore, we can consider that residues 1−4 are close to the 29−32 strand. Large $^3J_{HN-H\alpha}$ coupling constant values were obtained for most of the residues in the β-sheet, confirming its structure. The Cys30 coupling constant is abnormally low (5 Hz), suggesting a distortion in the β-sheet structure. This was also observed for the cysteine at the equivalent position in AgTX2 (Krezel et al., 1995).

Four turns are found in the structure. The first one involves residues Arg5 and Gly6 for which a strong sequential NH*i*−NH*i*+1 effect is observed. In fact, it corresponds to the strongest interaction observed in this region. Furthermore, the small Hαi−NH*i*+1 interactions observed between residues Cys4 and Arg5 and between residues Arg5 and Gly6 associated with the large amide−α-proton coupling constant for residues Cys4 and Arg5 are in favor of a type II′ β-turn. The second turn involves residues Thr18 and Gly19 but is quite difficult to characterize due to amide proton chemical shift degeneracy of residues Gly19 and Cys20. The third turn involves residues Asn27 and Arg28 and was defined above as a type 1 β-turn. The last turn is found at residues Tyr33 and Gly34 and is part of the novel structural characteristic of this toxin. The lack of cross peaks in this region did not allow the identification of the turn type.

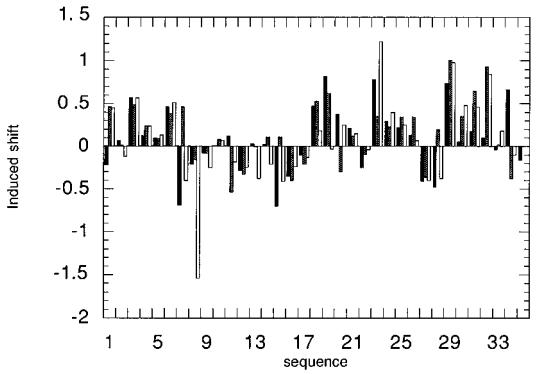

FIGURE 6: Induced shifts of the Hα protons of ChTX (white), NTX (dotted), and Pi1 (black). Induced shifts are deviations of the measured chemical shifts from the random coil values listed in Wishart et al. (1995).

In order to characterize further the overall structure of the Pi1 toxin, the deviations from the random coil position of the Hα and the NH chemical shifts were analyzed using the chemical shift index method (Wishart et al., 1992). The Hα and NH chemical shifts exhibit upfield shifts with respect to the random coil values in a helical conformation and downfield shifts in a β-strand extended conformation. The results for Hα protons are in reasonably good agreement with what is expected from other NMR parameters (Figure 6). The α-helical structure is observed between residues 7 and 17, while a β-strand is formed by stretches of residues 23−26 and 29−32 and to some extent between residues 2 and 4. The presence of two prolines, and in particular the Pro13 in the middle of the α-helix, could explain the deviation observed with the chemical shift index method for neighboring residues although this was taken into account for the calculation (Wishart et al., 1995).

Due to the limited quantity of sample available it was not possible to measure the proton−deuterium exchange of amide groups. Instead, the changes in the amide proton chemical shifts were monitored to evaluate the accessibility of these protons to solvent molecules (Kopple et al., 1969; Ohnishi & Urry, 1969). The variations studied in the temperature range from 25 to 40 °C are reported in Table 1. The backbone amide protons of the Pi1 toxin have highly variable temperature coefficients ranging from 0 to −7.7 ppb/°C. In particular, the temperature coefficients are very low, in the range of −3 ppb/°C, from residues Asp9 to Cys20, which are in the α-helical part of the toxin whereas an alternance of low- and high-temperature coefficients is observed in the β-strands. Indeed, the amide protons facing each other in the 22−26 and 29−32 β-strands, namely, the

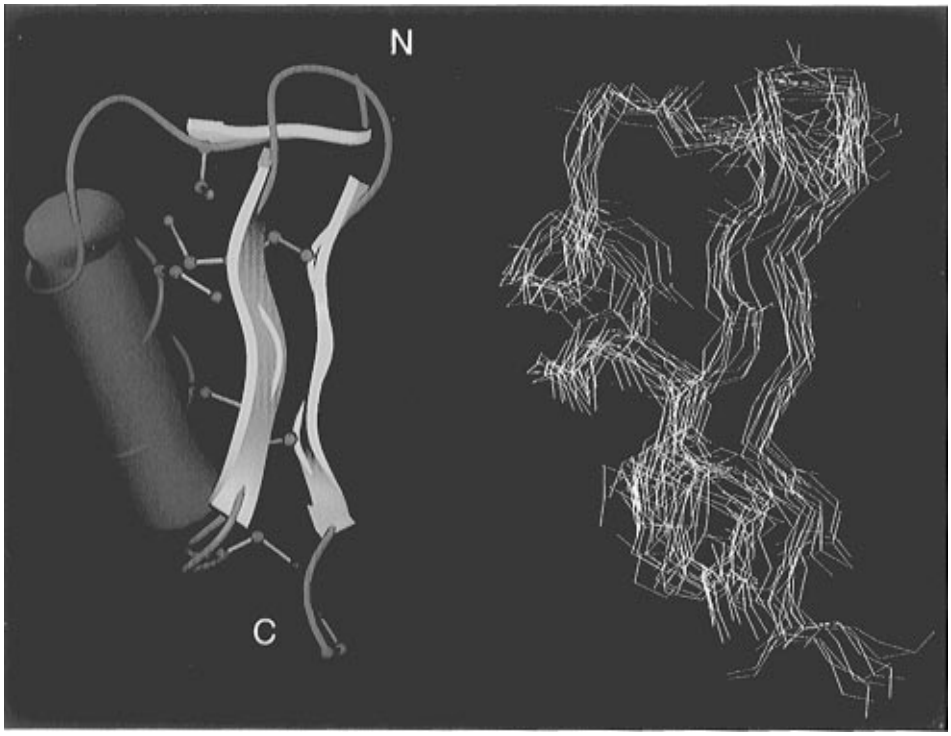

FIGURE 7: Schematic representation of the structure of Pi1 toxin with backbone superposition of the ten best calculated structures (right) (InsightII, Biosym/MSI).

amide protons of residues 24, 26, 29, and 31, have low coefficients whereas the coefficients of all other amide protons are substantially higher. In addition, the amide proton of Cys4, which has been found to exhibit a dipolar interaction with the Met29 Hα proton, also displays a low coefficient. If we consider that only very low coefficients (<2 ppb/°C) can be indicative of hydrogen bond formation (Temussi et al., 1987; Di Blasio et al., 1989), 11 hydrogen bonds can be proposed on the basis of such analysis (Table 1).

Although disulfide bridges were identified independently, a few interactions observed between cysteine Hβ protons confirmed those between cysteines 10−30 and cysteines 14−32. Others could not be detected. These are probably more flexible as has been seen already for several other toxins, such as the noxiustoxin (Dauplais et al., 1995). Finally, a few long-range interactions, such as those observed between Thr7 and Cys25 and between Thr18 and Tyr33, provide additional constraints for the three-dimensional structure determination.

Tertiary Structure. The distance and dihedral angle information derived from NOE cross-peak intensities and $^3J_{NH-H\alpha}$ values was used to construct a 3D model structure of the Pi1 toxin using the DIANA and DISCOVER programs.

The overall representation of the Pi1 structure is shown in Figure 7 together with backbone atom superposition of the ten best calculated structures. As expected from the number of available restraints, the calculated structures do not represent a highly converging family, and the global backbone atom RMSD calculated between all pairs of the ten structures equals 1.27 ± 0.23 Å. However, regular secondary structure elements, namely, an α-helix spanning the region of residues 8−17 and an antiparallel β-sheet formed by two strands running from residue 22 to residue 26 and from residue 29 to residue 33, respectively, are better defined. A global RMSD calculated over these three regions amounted to 1.06 ± 0.29 Å.

Although the N-terminal stretch of residues is not very well defined, an analysis of the Ramachandran angles confirms the existence of the β conformation between residues 2 and 4 followed by the α-helix spanning residues 7−17. For most calculated structures the turn linking these two elements seems to be consistent with a β type I rather than the type II′ suggested by directly measured NMR parameters. The positioning of the helix with respect to the antiparallel β-sheet is stabilized by two disulfide bridges between residues 10−30 and 14−32.

The large loop connecting the helix to the first strand of the antiparallel β-sheet contains a stretch of at least three residues with dihedral angles compatible with a β extended chain conformation. The first β-strand of the C-terminal β-sheet is inverted by a well-defined type I β-turn centered around residues 28 and 29, in agreement with the experimental data.

In most of the calculated structures the aromatic ring of Tyr33 lies above the Lys31 side chain as predicted by the upfield shifts observed for some of the Lys31 side chain protons.

DISCUSSION

The overall structure of Pi1 is characterized by a helix linked to a two-stranded β-sheet by two disulfide bridges, 10−30 and 14−32, through the consensus sequence ^{10}Cys-x-x-x-^{14}Cys on the helix and ^{30}Cys-x-^{32}Cys on the β-sheet. Despite some divergence in the primary sequence and the presence of an additional disulfide bridge, Pi1 exhibits the same basic structural motif found in ChTX (Bontems et al., 1992), IbTX (Johnson & Sugg, 1992), NTX (Dauplais et al., 1995), KTX (Fernandez et al., 1994), and MgTX (Johnson et al., 1994). As already observed for other toxins such as NTX, IBTX, KTX, and MgTX, the lack of interstrand

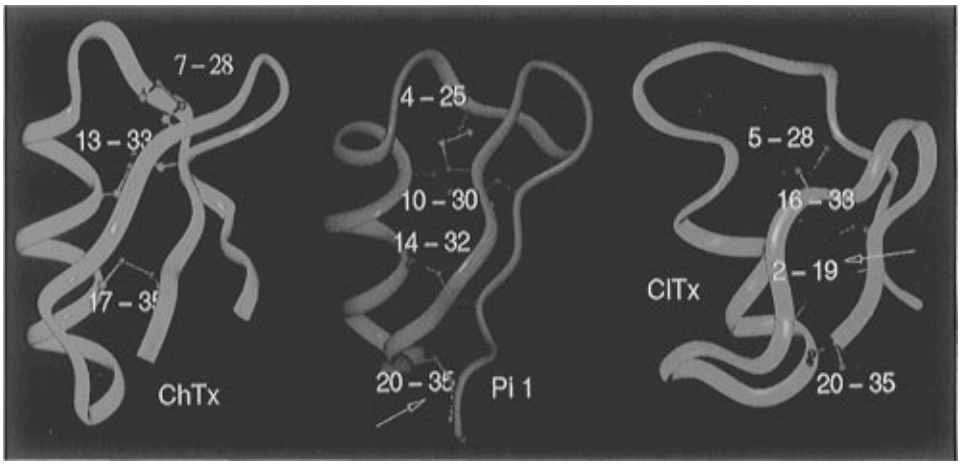

FIGURE 8: Comparison of the Pi1 structure (middle) with those of ChTX (left) [from Bontems et al. (1992); PDB code, 2crd] and ClTX (right) [from Lippens et al. (1995); PDB code, 1chl]. Disulfide bridges are shown, and additional disulfide bridges in Pi1 and in ClTX are indicated by arrows (InsightII, Biosym/MSI).

connectivity with the N-terminal part of the molecule can be interpreted in favor of an extended conformation for fragment 1−4 positioned close to the 29−32 β-strand.

The assignment of the Pi1 toxin proton resonances was compared with those of ChTX (Bontems et al., 1991a, 1992), NTX (Dauplais et al., 1995), KTX (Fernandez et al., 1994), MgTX (Johnson et al., 1994), and AgTX2 (Krezel et al., 1995). As the Pi1 toxin shares relatively low primary sequence similarity with other potassium channel toxins, the comparison was made between the shifts observed for Hα protons. These are more directly related to the secondary structure elements (Figure 6). The diagram shows that the conformational shifts are very similar and that the largest differences are observed either in the region around the extra disulfide bridge at position 20−35 or at the level of the α-helix, probably due to the presence of a proline in some of these toxins (KTX, NTX, and Pi1 and two for MgTX).

The presence of proline residues in the highly conserved helical region seems to be a constant for toxins that exhibit a high blockage activity of voltage-dependent potassium channels (NTX, MgTX, CllTX1, CllTX2, TsKα, AgTX, and KTX) (Fernandez et al., 1994; Rogowski et al., 1994) when compared to the high-conductance Ca^{2+}-activated K^+ channel toxins. All the toxins active on voltage-dependent potassium channels possess two highly conserved prolines, one in position $i-2$ or $i-3$ (residue 11 of ChTX) with respect to the helical Cys-$X_1X_2X_3$-Cys motif and the second in position X_3 (residue 16 of ChTX) of the same motif; MgTX and CllTX2 have a third proline in position X_2. For all of these toxins the first proline at position 11 (ChTX numbering) determines the beginning of the helix and therefore causes a reduction of the helix length by two residues as compared to ChTX. Pi1 lacks this first proline at the begining of the helix. The second, Pro16 (ChTX numbering) inserted in the helical part of the molecule, introduces some distortions. Calculations have shown that the presence of Pro is not unfavorable for helix formation as previously believed and that conformational change of only one residue is necessary to accommodate a proline in a distorted helix (Piela et al., 1987; Woolfson et al., 1990; MacArthur et al., 1991; Polinsky et al., 1992). It has been suggested that the conservation of these Pro residues might have a functional role in determining selectivity (Fernandez et al., 1994).

In comparison with other toxins, which display differential activities toward K^+ channels, the helix of Pi1 spans 11 residues. Helix length varies from 7 residues in KTX to 10 residues in ChTX, MgTX, and IbTX and to 11 residues in NTX. The β-sheet of Pi1 might be implicated in the capacity of Pi1 to recognize voltage-dependent K^+ channels. The region from 23 to 32 forms a hairpin structure of the same length as that of ChTX but shorter than that of IbTX or AgTX2 (25−36) and MgTX or NTX (25−38). It has already been suggested that the longer sheet may have implications for channel selectivity in MgTX (Johnson et al., 1994; Stampe et al., 1994). The Pi1 folding does not affect the accessibility of Lys24 (Lys27 in ChTX), a residue shown to be essential for tight binding of ChTX to the channel receptor (Park & Miller, 1992) and known to interact with potassium ions in the channel conduction pathway (Golstein & Miller, 1993; Naini & Miller, 1996).

The Pi1 primary structure shows a number of differences when compared to structures of other known peptides that recognize potassium channels. The ^{26}Gly-X-Cys^{28} (ChTX numbering) pattern of the previously proposed consensus sequence is not preserved in Pi1 (Bontems et al., 1991b; Krezel et al., 1995) (Figure 1). Two residues, the lysine (32 in ChTX) and the glycine (26 in ChTX), thought to be part of the consensus sequence and present in all other toxins are replaced by a methionine at position 29 and a serine at position 23 in Pi1. It was proposed that a glycine was required at position 26 in ChTX due to the lack of local space in the contact area of the helix and the β-sheet (Bontems et al., 1991b). The presence of the 20−35 disulfide bridge in Pi1 has increased the limited space at the intersection of the helix and the sheet allowing the insertion of a larger side chain. Pi1 is not the only case for which the consensus sequence is not entirely preserved. Indeed, in NTX and MgTX the consensus sequence comprises an additional alanine residue, at position $i-2$ to the cysteine 28 (Johnson et al., 1994) while in ClTX1 there is an additional Gly at this position (Martin et al., 1994). In Figure 8 are shown the structure of the *Pandinus* toxin compared with those of the charybdotoxin and the chlorotoxin. Although the proposed role of the additional disulfide bridge in the chlorotoxin was to replace a hydrophobic contact between two valine residues present in the charybdotoxin (Lippens et al., 1995), this is not the case in the *Pandinus* toxin.

The eight most important residues involved in interaction with the channel in the charybdotoxin-like toxins (forming

the calcium-activated potassium channel group) are not strictly conserved in *Pandinus*. Indeed, the binding assay results suggest that the toxin is likely to belong to the noxiustoxin-like group, i.e., that of the the voltage-gated potassium channel type (Olamendi-Portugal et al., 1996). The mutational analysis of binding of ChTX- to BK-type channels demonstrated the importance of eight residues: Ser10, Trp14, Arg25, Lys27, Met29, Asn30, Arg34, and Tyr36 (Stampe et al., 1994). Five of these residues (Lys27, Met29, Asn30, Arg34, and Tyr36) were shown to be critical for the recognition of a voltage-dependent K^+ channel (shaker) by ChTX (Golstein et al., 1994). Examination of the amino acid sequences of ChTX and Pi1 reveals that these five residues are present in both toxins with a conservative mutation Arg34 (ChTX) into Lys31(Pi1) whereas the three other residues crucial for binding of ChTX to BK are absent in Pi1. Two of the residues are located in the helix (Ser10 and Trp14) and the third one (Arg25) appears at the base of the β-sheet. Finally, Pi1 has a net positive charge of +5 which is the same as in the other toxins and its charge distribution is quite similar.

Sequence alignment of voltage-gated potassium channel specific scorpion toxins (Figure 1) shows that several residues are very well conserved in the sequence (upper line in bold letters, ChTX numbering) leading to the following consensus for voltage-dependent potassium channel toxins:

^{3}**I**-^{5}**V**-^{7}**C**--^{10}**S**^{11}**P**^{12}**Q**^{13}**C**--^{16}**P**^{17}**C**^{18}**K** ^{26}**G**^{27}**K**^{28}**C**^{29}**I/M**^{30}**N**-^{32}**K**^{33}**C**±^{35}**C**

L- V- C-- T S D C-- P C K S K C I N- M C± C

It is interesting to note that the strictly conserved residues are adjacent to the cysteines. The Asn30 residue (ChTX numbering) shown to be important for the two types of voltage-dependent channels and present in all the short-chain scorpion toxins binding the Kv1.3 channel (NTX, MgTX, ChTX, KtX, AgTX1,2,3) is also present in Pi1. Similarly, as in NTX, Asn27 of Pi1 is located at position $i-1$ of the β-turn (Dauplais et al., 1995). Finally, the only nonconservative replacements in Pi1 (lower line) are found at positions 11, 12, 26, and 32 (ChTX numbering). It is too early yet to estimate the biological implications of these natural mutations.

In conclusion, we have shown in this paper that it is possible to collect a sufficient data set with nanomole amounts of product and obtain a reasonable structure of the toxin using the new technology offered by the nano-NMR probe. There are advantages to using a nano-NMR probe for study of such a small molecule that can be synthesized. These are as follows: first, the presence of numerous disulfide bridges can render difficult the synthesis of these small toxins. Actually, primary sequences of several of these small toxins have been known for many years, sometimes decades; however, their structures have been solved only recently, charybdotoxin being the first one (Bontems et al., 1991a,b). Second, even when the synthesis is performed successfully, it is still important to know if the compound synthesized is identical to the native one. The technique we have reported here, although certainly not the only one possible, gives a considerable amount of structural information, and yet, it has been obtained with a scarce quantity of material.

Recently, the three-dimensional structure of maurotoxin has been reported (Blanc & Darbon, 1996). This small basic protein isolated from the venom of the tunisian Chactoides *Scorpio maurus* has 34 amino acids and is active on both small-conductance calcium-activated and voltage-gated potassium channels. Like Pi1, the maurotoxin is cross-linked by four disulfide bridges, and despite the striking homology between the two toxins the disulfide bond pairing differs: pairings 14−32 and 20−35 in Pi1 are replaced by 14−20 and 32−35 (Pi1 numbering) in maurotoxin. In one case, Pi1, the disulfide bridges were determined on the native toxin whereas in the maurotoxin this was done on the synthetic toxin (Leblanc and Darbon, personal communication). The spatial proximity of the height cysteines renders difficult the determination of the disulfide pairing from NMR data only. However, the different disulfide pairings observed for the two toxins should lead to different thermal stability. Assuming both results are correct (this paper and the Blanc and Darbon communication), this raises an interesting question with regard to protein folding.

At a time when there is a trend of going toward ultra-high-field spectrometers, reduction of the sample size can be seen as an alternative, in particular in biological applications. Recently published work on nanoliter volume samples provides a good example of such a promising approach (Olson et al., 1995).

ACKNOWLEDGMENT

We thank M. Sc. Timoteo Olamendi-Portugal for the purification of Pi1 toxin. As we do not have a nano-NMR probe in our Laboratory, experiments have been carried out at different places and we would like to thank the following people: the Varian Team at Darmstadt, Dr. Paul Kiefer (Varian Palo-Alto), Dr. Simone Mergui, and Vincent Ronfle (Varian France) for the lending of the probe and Dr. Claude Morat and Marie-Christine Brochiez at Grenoble for giving us access to the nano-NMR probe. We are indebted to Dr. Bernard Gilquin for valuable discussions. The DIANA software was kindly provided by Prof. K. Wüthrich.

SUPPORTING INFORMATION AVAILABLE

Coordinates of the ten best structures of the potassium channel blocking toxin from the scorpion *P. imperator* (59 pages). Ordering information is given on any current masthead page.

REFERENCES

Barbara, T. M. (1994) *J. Magn. Reson., Ser. A 109*, 265−269.
Bax, A., & Davis, D. G. (1985) *J. Magn. Reson. 65*, 355−360.
Blanc, E., & Darbon, H. (1996) Proceedings of the 13th European Experimental NMR Conference, May 19−24, Paris.
Blaustein, M. P., Rogowski, R. S., Schneider, M. J., & Krueger, B. K. (1991) *Mol. Pharmacol. 40*, 932−942.
Bontems, F., Roumestand, C., Gilquin, B., Menez, A., & Toma, F. (1991a) *Science 254*, 1521−1523.
Bontems, F., Roumestand, C., Boyot, P., Gilquin, B., Doljansky, Y., Menez, M., & Toma, F. (1991b) *Eur. J. Biochem. 196*, 19−28.
Bontems, F., Gilquin, B., Roumestand, C., Menez, A., & Toma, F. (1992) *Biochemistry 31*, 7756−7764.
Boyd, J., Dobson, C. M., & Redfield, C. (1983) *J. Magn. Reson. 55*, 170−176.
Brünger, A. T. (1992) *X-PLOR version 3.1: A System for X-Ray Crystallography and NMR*, Yale University Press, New Haven and London.
Calderon-Aranda, E. S., Olamendi-Portugal, T., & Possani, L. D. (1995) *Vaccine 13*, 1198−1206.
Carbone, E., Wanke, E., Prestipino, G., Possani, L. D., & Maelicke, A. (1982) *Nature 296*, 90−91.
Catterall, W. A. (1980) *Annu. Rev. Pharmacol. Toxicol. 20*, 15−43.

Clore, G. M., Nilges, M., Sukumaran, D. K., Brunger, A. T., Karplus, M., Easthope, P., & Havel, T. F. (1986) *EMBO J. 5*, 2729−2735.
Crest, M., Jacquet, G., Gola, M., Zerouk, H., Benlismane, A., Rochat, H., Mansuelle, P., & Martin-Eauclaire, M.-F. (1992) *J. Biol. Chem. 267*, 1640−1647.
Darbon, H., Weber, C., & Braun, W. (1991) *Biochemistry 30*, 1836−1845.
Daubert-Osguthorpe, P., Roberts, V. A., Osguthorpe, D. J., Wolff, J., Genest, M., & Hagler, A. T. (1988) *Proteins: Struct., Funct., Genet. 4*, 31−47.
Dauplais, M., Gilquin, B., Possani, L. D., Gurrola-Briones, G., Roumestand, C., & Menez, A. (1995) *Biochemistry 34*, 16563−16573.
Debin J. A., Maggio, J. E., & Strichartz, G. R. (1993) *Am. J. Physiol.* (*Cell Physiol. 33*) *264*, 361−369.
Dent, M. A. R., Possani, L. D., Ramirez, G. A., & Fletcher, P. L., Jr. (1980) *Toxicon 18*, 343−350.
Di Blasio, B., Rossi, F., Benedetti, E., Pavone, V., Pedone, C., Temussi, P. A., Zanotti, G., & Tancredi, T. (1989) *J. Am. Chem. Soc. 111*, 9089−9098.
Fazal, A., Beg, O. V., Shafgat, J., Zaidi, Z. H., & Jornvall, H. (1989) *FEBS Lett. 257*, 260−262.
Fernandez, I., Romi, R., Szendeffy, S., Martin-Eauclaire, M.-F., Rochat, F., Van Rietschoten, J., Pons, M., & Giralt, E. (1994) *Biochemistry 33*, 14256−14263.
Galvez, A., Gimenez-Gallego, G., Reuben, J. P., Roy-Contencin, L., Feigenbaum, P., Kaczorowski, G. J., & Garcia, M. L. (1990) *J. Biol. Chem. 265*, 11083−11090.
Garcia, M. L., Garcia-Calvo, M., Hidalgo, P., Lee, A., & Mackinnon, R. (1994) *Biochemistry 33*, 6834−6839.
Garcia-Calvo, M., Leonard, R. J., Novick, J., Stevens, S. P., Schmalhofer, W., Kaczorowski, G. J., & Garcia, M. L. (1993) *J. Biol. Chem. 268*, 18886−18874.
Gimenez-Gallego, G., Navia, M. A., Reuben, J. P., Katz, G. M., Kaczorowski, G. J., & Garcia, M. L (1988) *Proc. Natl. Acad. Sci. U.S.A. 85*, 3329−3333.
Golstein, S. A. N., & Miller, C. (1993) *Biophys. J. 65*, 1613−1619.
Golstein, S. A. N., Pheasant, D. J., & Miller, C. (1994) *Neuron 12*, 1377−1388.
Griesinger, C., Wüthrich, K., & Ernst, R. R. (1988) *J. Am. Chem. Soc. 110*, 7870−7892.
Grishin, E. V., Soldatov, N. M., Tashmuchamedov, B. A., & Atakuziev, B. U. (1978) *Bioorg. Khem. (USSR) 4*, 450−461.
Güntert, P., & Wüthrich, K. (1991) *J. Biomol. NMR 1*, 447−456.
Güntert, P., Braun, W., & Wüthrich, K. (1991) *J. Mol. Biol. 217*, 517−530.
Johnson, B. A., & Sugg, E. E. (1992) *Biochemistry 31*, 8151−8159.
Johnson, B. A., Stevens, S. C., & Williamson, J. M. (1994) *Biochemistry 33*, 15061−15070.
Krezel, A. M., Kasibhatla, C., Hidalgo, P., MacKinnon, R., & Wagner, G. (1995) *Protein Sci. 4*, 1478−1489.
Kobyashi, Y., Takashima, H., Tamaoki, H., Kiogoku, Y., Lambert, P., Kuroda, H., Chino, N., Watanabe, T. X., Kimura, T., Sakakibara, S., & Moroder, L. (1991) *Biopolymers 31*, 1213−1220.
Kopeyan, C., Martinez, G., Lissitzky, S., Miranda, F., & Rochat, H. (1974) *Eur. J. Biochem. 47*, 483−489.
Kopple, K. D., Onishi, M., & Go, A. (1969) *J. Am. Chem. Soc. 91*, 4264−4275.
Kumar, A., Ernst, R. R., & Wüthrich, K. (1980) *Biochem. Biophys. Res. Commun. 95*, 1−6.
Lazdunski, M., Frelin, Ch., Barhanin, J., Lombet, A., Meiri, H., Pauron, D., Romey, G., Schmid, A., Schweitz, H., Vigne, P., & Vijverberg, H. P. M. (1986) in *Tetrodotoxin, saxitoxin and the molecular biology of the sodium channels* (Kao, C. Y., & Levinson, S. R., Eds.) Vol. 479, pp 204−220, New York Academy of Sciences, New York.
Lippens, G., Najib, J., Wodak, S. J., & Tartar, A. (1995) *Biochemistry 34*, 13−21.
Lucchesi, K., Ravindran, A., Young, H., & Moczydlowski, E. (1989) *J. Membr. Biol. 109*, 269−281.
MacArthur, M. W., & Thornton, J. M. (1991) *J. Mol. Biol. 218*, 397−412.
Manzi, A., Salimath, P. V., Spiro, R. C., Keifer, P. A., & Freeze, H. H. (1995) *J. Biol. Chem. 270*, 9154−9163.
Marion, D., & Bax, A. (1988) *J. Magn. Reson. 80*, 528.
Martin, B. M., Ramirez, A. N., Gurrola, G. B., Nobile, M., Prestipino, G., & Possani, L. D. (1994) *Biochem. J. 304*, 51−56.
Menez, A., Bontems, F., Roumestand, C., Gilquin, B., & Toma, F. (1992) *Proc. R. Soc. Edinburgh 99B*, 83−103.
Meunier, S., Bernassau, J. M., Sabatier, J. M., Martin-Eauclaire, M. F., Van Rietschoten, J., Cambillau, C., & Darbon, H. (1993) *Biochemistry 32*, 11969−11976.
Meves, H., Marc, S., & Watt, D. (1986) in *Tetrodotoxin, saxitoxin and the molecular biology of the sodium channels* (Kao, C. Y., & Levinson, S. R., Eds.) Vol. 479, pp 113−132, New York Academy of Sciences, New York.
Miller, C. (1995) *Neuron 15*, 5−10.
Miller, C., Moczydlowski, E., Latorre, R., & Phillips, M. (1985) *Nature 313*, 316−318.
Moczydlowski, E., Lucchesi, K., & Ravindran, A. (1988) *J. Membr. Biol. 105*, 95−111.
Mozurkewich, G., Ringermacher, H. I., & Bolef, D. I (1979) *Phys. Rev. B 20*, 33−38.
Naini, A. A., & Miller, C. (1996) *Biochemistry 35*, 6181−6187.
Nilges, M., Gronenborn, A. M, Brünger, A. T., & Clore, G. M. (1988) *Protein Eng. 2*, 27−38.
Ohnishi, M., & Urry, D. W. (1969) *Biochem. Biophys. Res. Commun. 36*, 194−202.
Olamendi-Portugal, T., Gomez-Lagunas, F., Gurrola, G. B., & Possani, L. D. (1996) *Biochem. J. 315*, 977−981.
Olson, D. L., Peck, T. L., Webb, A. G., Magin, R. L., & Sweedler, J. V. (1995) *Science 270*, 1967−1970.
Pardi, A., Billeter, M., & Wüthrich, K. (1984) *J. Mol. Biol. 180*, 741−751.
Park, C. S., & Miller, C. (1992) *Neuron 9*, 307−313.
Piela, L., Nemethy, G., & Scheraga, H. A. (1987) *Biopolymers 26*, 1587−1600.
Polinsky, A., Goodman, M., Williams, K. A., & Deber, C. M. (1992) *Biopolymers 32*, 399−406.
Possani, L. D. (1984) in *Handbook of Natural Toxins* (Tu, A. T., Ed.) Vol. 2, pp 513−550, Marcel Dekker, Inc., New York.
Possani, L. D., Martin, B. M., & Svendsen, I. (1982) *Carlsberg Res. Commun. 47*, 285−289.
Rochat, H., Bernard, P., & Couraud, F. (1979) in *Advances in Cytopharmacology* (Ceccarelli, B., & Clementi, F., Eds.) Vol. 3B, pp 325−334, Raven Press, New York.
Rogowsky, R. S., Krueger, B. K., Collins, J. H., & Blaustein, M. P. (1994) *Proc. Natl. Acad. Sci. U.S.A. 91*, 1475−1479.
Sissom, W. D. (1990) in *The Biology of Scorpions* (Polis, G. A., Ed.) Stanford University Press, Stanford, CA.
Sodano, P., & Delepierre, M. (1993) *J. Magn. Reson., Ser. A 104*, 88−92.
Stampe, P., Kolmakova-Partensky, L., & Miller, C. (1994) *Biochemistry 33*, 443−450.
States, D. J., Haberkorn, R. A., & Rubens, D. J. (1982) *J. Magn. Reson. 48*, 286−292.
Temussi, P. A., Tancredi, T., Pastore, A., & Castiglione-Morelli, M. A. (1987) *Biochemistry 26*, 7856−7863.
Valdivia, H. H., Kirby, M. S., Lederer, W. J., & Coronado, R. (1992) *Proc. Natl. Acad. Sci. U.S.A. 89*, 12185−12189.
Wagner, G., Braun, W., Havel, T. F., Schaumann, T., Go, N., & Wüthrich, K. (1987) *J. Mol. Biol. 196*, 611−639.
Wishart, D. S., Sykes, B. D., & Richards, F. M. (1992) *Biochemistry 31*, 1647−1651.
Wishart, D., Bigam, C. G., Holm, A., Hodges, R. S., & Sykes, B. D. (1995) *J. Biomol. NMR 5*, 67−81.
Woolfson, D. N., & Williams, D. H. (1990) *FEBS Lett. 277*, 185−188.
Wüthrich, K. (1986) *NMR of Proteins and Nucleic Acids*, John Wiley and Sons, New York.
Zlotkin, E., Miranda, F., & Rochat, H. (1978) in *Handbook of Experimental Pharmacology, Athropod venoms* (Bettini, S., Ed.) Vol. 48, pp 317−369, Springer-Verlag, Berlin.

BI9617116